Food Hydrocolloids 23 (2009) 1864–1876

Contents lists available at ScienceDirect

Food Hydrocolloids

journal homepage: www.elsevier.com/locate/foodhyd

Physico-chemical factors controlling the foamability and foam stability of milk proteins: Sodium caseinate and whey protein concentrates

Krastanka G. Marinova [a,*], Elka S. Basheva [a], Boriana Nenova [a], Mila Temelska [a], Amir Y. Mirarefi [b], Bruce Campbell [b], Ivan B. Ivanov [a]

[a] Laboratory of Chemical Physics & Engineering, Faculty of Chemistry, Sofia University, 1 James Bourchier Ave., 1164 Sofia, Bulgaria
[b] Kraft Foods Global Inc., Technology Center, 801 Waukegan Road, Glenview, IL 60025, U.S.A

ARTICLE INFO

Article history:
Received 30 December 2008
Accepted 12 March 2009

Keywords:
Foam
Sodium caseinate
Whey protein concentrate
Protein adsorption
pH dependence

ABSTRACT

We explored the foaming behavior of the two main types of milk proteins: flexible caseins and globular whey proteins. Direct foam comparison was complemented with measurements in model experiments such as thin foam films, dynamic surface tension, and protein adsorption. Foaming was studied as a function of pH (from below to above isoelectric point, pI) and range of ionic strengths. Maximum foamability was observed near pI ≈ 4.2 for WPC in contrast to sodium caseinate which had minimum foaming near pI = 4.6. Good foamability behavior correlated well with an increased adsorption, faster dynamic surface tension decrease and increased film lifetime. Differences in the stability of the foams and foam were explained with the different molecular structure and different aggregation behavior of the two protein types. Far from its isoelectric pI, casein adsorption layers are denser and thicker thus ensuring better stabilization. Added electrolyte increased further the adsorption and the repulsion between the surfaces (probably by steric and/or osmotic mechanism). In contrast the globular molecules of WPC probably could not compact well to ensure the necessary films and foams stabilization far from pI, even after electrolyte addition.

1. Introduction

1.1. Milk proteins as foam and emulsion stabilizers

Milk proteins are widely used for stabilization of various food products including foamed ones (Dickinson & Patino, 1999; Möbius & Miller, 1998). Therefore the foaming of solutions containing different milk proteins has been studied under various conditions (see for example Lee, Morr, & Ha, 1992; Martin, Grolle, Bos, Cohen Stuart, & van Vliet, 2002; Morr, 1985; Murray, 2007; Patino, Sanchez, & Nino, 2008; Saint-Jalmes, Peugeot, Ferraz, & Langevin, 2005; Sanchez & Patino, 2005). Despite the wide usage and exhaustive studies of the protein foams, and of the surface (starting from the works by Graham & Phillips, 1979, 1980) and bulk protein properties, there are a number of open questions left due to the complexities inherent to proteins and foams (Murray, 2007; Patino, Sanchez, & Nino, 2008).

Milk proteins can be classified in two groups according to their structure (Creamer & MacGibbon, 1996; Dickinson & Patino, 1999): flexible and globular. Flexible caseins have no tertiary structure and include proteins α_{S1}-, α_{S2}-, β- and κ-casein, the mixtures sodium caseinate, calcium caseinate, acid casein, etc. Globular proteins which can be isolated after casein precipitation (e.g. in the process of cheese making) are called whey proteins. These proteins contain disulphide bridges, tertiary structure, and preserve their globular molecular shape even after adsorption on an interface. Due to the different molecular structure, the two types of proteins form different in structure adsorption layers (Dickinson, 1999; Dickinson, Horne, Phipps, & Richardson, 1993; Graham & Phillips, 1979, 1980; Pereira, Johansson, Radke, & Blanch, 2003) with very different surface rheological properties (Benjamins, Cagna, & Lucassen-Reynders, 1996; Graham & Phillips, 1979, 1980). In spite of these known differences, a convincing explanation for the differences in the foaming and emulsifying properties of the two protein types is still missing in the literature.

Protein molecules change their charging and surface activity with pH and accordingly their foamability and emulsifying properties are also altered. Many authors have studied the surface behavior of different proteins at fixed pH (usually near or equal to 7, see Benjamins et al., 1996; Graham & Phillips, 1979, 1980; Sanchez & Patino, 2005; Tcholakova, Denkov, Ivanov, & Campbell, 2002) with their focus on adsorption on interfaces (Gurkov, Russev, Danov,

* Corresponding author. Tel.: +359 2 962 5310; fax: +359 2 962 5643.
E-mail address: KM@LCPE.UNI-SOFIA.BG (K.G. Marinova).

0268-005X/$ – see front matter © 2009 Elsevier Ltd. All rights reserved.
doi:10.1016/j.foodhyd.2009.03.003

Ivanov, & Campbell, 2003; Makievski et al., 1998; Russev, Arguirov, & Gurkov, 2000) and/or thin film behavior (Basheva, Gurkov, Christov, & Campbell, 2006; Dimitrova, Leal-Calderon, Gurkov, & Campbell, 2001; Marinova et al., 1997). Few studies describe the coalescence stability of protein stabilized foams (e.g. Refs. Lee et al., 1992; Martin et al., 2002; Morr, 1985) and emulsions (Masson & Jost, 1986; Tcholakova, Denkov, Ivanov, & Campbell, 2006; Tcholakova, Denkov, Sidzhakova, Ivanov, & Campbell, 2005) in broader pH ranges. For example, Tcholakova et al. (2006, 2005) have found that the stability of BLG emulsions is lower at the isoelectric pH as compared to that at the natural pH = 6.2, despite the higher adsorption at pI. For WPC emulsions Masson and Jost (1986) have determined that the mean particle size and width of the size distribution is largest near pI. Still studies satisfactorily relating the observed physico-chemical properties of caseins and whey proteins to their foaming and emulsifying capacity in a pH range above and below their isoelectric points are missing.

In this paper we systematically investigate the factors affecting foamability and foam stability of solutions of the two basic milk proteins: sodium caseinate and whey protein. The pH was varied in the range from 3 to 6.8 (from below to above the isoelectric point). Effect of electrolyte NaCl was also explored. Several comparative measurements were performed with the pure proteins β-casein and β-lactoglobulin. β-casein was chosen because its surface properties have been found to be very similar to those of Na-caseinate (Sanchez & Patino, 2005); β-lactoglobulin was chosen because it is the main component of the whey protein concentrates.

1.2. Factors affecting the foamability and foam stability

The intricacy of the food foams results not only from the complicated structure of the used proteins but also from the complexity of the foams as dispersions. While simply defined as dispersions of gas in a liquid (Bikerman, 1973; Exerowa & Kruglyakov, 1998; Prud'homme & Khan, 1996; Weaire & Hutzler, 1999), foams can be stabilized with variety of low and high molecular weight surface active substances and/or solid particles, which physico-chemical properties (structure, rate of adsorption, interactions, etc.) further determine the properties of the foam itself. In addition, the process of foam formation depends on the properties of the used stabilizing substances and on the particular procedure used for foam formation.

Bubbling and stirring are the two main categories of mechanical methods for foam formation (Bikerman, 1973; Exerowa & Kruglyakov, 1998; Prud'homme & Khan, 1996; Weaire & Hutzler, 1999). In the bubbling methods the foam is generated by bubbling gas through the foaming solution. Bubbling can be realized through a single capillary, a set of capillaries, or a porous plate placed in the lower part of the foam generator. The bubbles released from the pores float up under the effect of buoyancy. The size of the foam bubbles produced in this way generally depend on (i) the pore size; (ii) physico-chemical properties of the surfactant solution (e.g. equilibrium or dynamic surface tension, surface elasticity, bulk viscosity, etc.); (iii) conditions of foam formation, i.e. rate of gas flow, temperature, etc. Depending on the gas flow rate one can distinguish two basic regimes of bubbles and foam formation – "dynamic" and "quasi-static" (some authors report three or four regimes (Exerowa & Kruglyakov, 1998; Gerlach, Alleborn, Buwa, & Durst, 2007; Weaire & Hutzler, 1999)). In the stirring methods foam is generated by mechanical mixing of the gas and liquid phases, e.g. by whipping or by mixing with a stirrer, by shaking a vessel partially filled with solution, by simultaneous flow of gas and liquid in a tube, by pouring liquid on the surface of the same solution, etc. It is simpler to define the mechanical conditions in the bubbling methods, hence those methods are often used in the quantitative studies (Prud'homme & Khan, 1996; Weaire & Hutzler, 1999). Whatever the foaming method is, the foaming capacity (or foamability) of a given solution is defined through the volume of the formed foam under fixed conditions (foaming time, temperature, stirring intensity, etc.) or through the time necessary to obtain a required volume.

In our studies we used two different mechanical methods for foam formation: bubbling and shaking of a closed cylinder. Thus we checked whether the hydrodynamic conditions affected the observed impact of the physico-chemical factors on the foamability and foam stability.

After a foam formation several processes occur each of them leading to foam destruction (Denkov, 2004; Denkov & Marinova, 2006; Murray & Ettellaie, 2004; Prud'homme & Khan, 1996): (i) liquid drainage; (ii) bubble coalescence; (iii) bubble disproportionation. Foam stability usually refers to the ability of the foam to maintain some of its properties constant with time (e.g. foam volume and/or bubble size and/or liquid content). Depending on the particular property and time scale of interest some of the above processes could be of major importance (Denkov & Marinova, 2006).

Drainage (gravitational separation or syneresis) can be considered as a rise of bubbles through the foam mass, while the liquid drains through the lamellae and through the Plateau borders between the bubbles under the effect of gravity (Denkov, 2004; Denkov & Marinova, 2006; Murray & Ettellaie, 2004; Prud'homme & Khan, 1996; Saint-Jalmes et al., 2005; Weaire & Hutzler, 1999).

Bubble coalescence represents a process of thinning and rupture of the thin liquid films separating two neighboring bubbles (or the film between the bubble and the ambient atmosphere). The main factors controlling the foam stability against coalescence are the colloidal surface forces, acting between the film surfaces, the adsorption of surface active molecules, the squeezing force pushing the bubbles against each other (i.e. the capillary pressure of the bubbles), the film diameter, etc. (Denkov, 2004; Denkov & Marinova, 2006; Exerowa & Kruglyakov, 1998; Ivanov, 1988, 2002; Pereira et al., 2003; Prud'homme & Khan, 1996).

Bubble–bubble coalescence occurs during foam formation as well and it is strongly affected by the dynamics of adsorption of the surface active molecules. Faster adsorption leads to more stable foam films under dynamic conditions and to suppressed coalescence of the bubbles during foaming (Denkov & Marinova, 2006; Ivanov, 2002). We have previously shown (Ivanov, 2002) that the lifetimes of bubbles and drops stabilized with non-ionic surfactants or proteins depend exclusively on the degree of coverage θ no matter how it was reached – at equilibrium or at a given moment of time after the start of the adsorption. Long-term stability was found at $\theta = 0.8$–0.9. The same threshold coverage was found to ensure the stability of emulsions as well (Tcholakova et al., 2006).

Disproportionation is the process of bubble coarsening due to gas diffusion across the foam films, from the smaller to the larger bubbles (Prud'homme & Khan, 1996; Weaire & Hutzler, 1999). This process does not lead to direct foam volume decrease but indirectly affects it since the larger bubbles contact through larger films and these films are easier to rupture (Ivanov, 1988). In the time-scale of our foam observations (15 min) the disproportionation was not found to have a significant impact on the overall foam volume stability.

In order to explore the particular role of the surface and thin films properties on the foamability and foam stability of the studied proteins we performed systematic measurements of protein adsorption, rate of surface tension decrease and thin film stability. Our aim was to outline the factors which govern foaming by these proteins and to clarify the specific role(s) of their molecular structure and interactions.

2. Materials and methods

2.1. Studied systems and used materials

We used the following proteins: sodium caseinate (hereafter noted as Na-cas, Alanate 185, NZMP, New Zealand), whey protein concentrate, (WPC, Hilmar 8000, Hilmar Ingredients, USA), whey protein isolate (WPI, Alacen 895, NZMP, New Zealand), β-casein (β-cas, from bovine milk, Sigma, cat. # C6905, Lot. # 105K7410), and β-lactoglobulin (BLG, from bovine milk, Sigma, cat. # L0130, Lot. # 095K7006). The concentration of the protein solution was varied from 0.001 to 5 wt%. pH of the solutions was varied from the natural (6.4 to 6.8 for the used proteins) down to 3. pH below the natural were adjusted by addition of 0.1 M HCl (hydrochloric acid, Merck). Electrolyte NaCl (sodium chloride, Merck) was added to some of the solutions.

All solutions were prepared with deionized water from Milli-Q system (Millipore, USA) and contained a preservative 0.1 g/l NaN_3 (sodium azide, Merck).

2.2. Foam studies

Foamability and foam stability of the solutions was studied by two methods, which differ by the process of foam generation: (i) a bubbling method which was realized with the Foamscan instrument (ITConcept, France); and (ii) a stirring/shaking method, which was realized by hand shaking of a closed cylinder containing the solution (and air). In details:

(i) In the Foamscan apparatus the foam was generated by sparging a gas through a porous frit in fixed amount of liquid (30 mL) at a preliminary defined gas flow rate for a fixed time or until fixed foam volume was formed. We applied a procedure with a fixed foam volume of 140 mL. We measured precisely the gas volume and flow rate, and the volume of the formed foam as a function of time. Measurements were performed with gas flow rates 50 or 100 mL/min. Glass frit with a porosity of 16–40 μm was used.

Measure for the foamability of the solutions in the Foamscan is the Foam capacity, FC, at the end of gas sparging, which is defined as:

$$\mathrm{FC} = V_{\mathrm{foam0}}/V_{\mathrm{gas}} \tag{1}$$

where V_{foam0} is the volume of the formed foam, and V_{gas} is the volume of the gas introduced for the formation of this foam. When the formed foam is not very stable and part of the introduced gas has been released due to bubbles bursting FC < 1. When the formed foam has been stable during formation (no bubble coalescence with the atmosphere) FC > 1.

The liquid content in the foam is characterized by the maximum foam density, MD:

$$\mathrm{MD} = V_{\mathrm{liq0}}/V_{\mathrm{foam0}} \tag{2}$$

where V_{liq0} is the volume of the liquid entrapped in the formed foam. In general a higher liquid content is indication for smaller bubble size and longer time for drainage, and possibly higher stability after formation (Koehler, Hilgenfeldt, & Stone, 2000; Murray & Ettellaie, 2004).

Foam stability is characterized by several parameters: Percentage volumetric foam stability, FVS%, and percentage liquid stability, FLS%, are defined as:

$$\mathrm{FVS\%} = \left(V_{\mathrm{foam}}/V_{\mathrm{foam0}}\right) \times 100, \quad \mathrm{FLS\%} = \left(V_{\mathrm{liq}}/V_{\mathrm{liq0}}\right) \times 100, \tag{3}$$

The volumes of the foam, V_{foam}, and of the entrapped liquid, V_{liq}, change with the time t. When the values of FVS% decrease to 50% one defines the foam half life-time $t_{\mathrm{foam1/2}}$. The time for drainage of the half of the initially entrapped liquid in the foam is $t_{\mathrm{liq1/2}}$.

In the Foamscan instrument one could measure the radius of the bubbles at a fixed height of the foam column. We determined and compared (see below) the mean radius of the bubbles, R_{B}, at a height of 5 cm above the liquid level in a series of experiments with Na-cas solutions.

(ii) In the Bartsch method (Bartsch, 1924), the foam was generated by 10 vigorous shakings by hand of a closed cylinder (75 mL total volume, graduated to 50 mL) containing 15 mL protein solution and 60 mL air.

The initial foam volume and the subsequent foam decay during 15 min (900 s) were monitored. The solution foamability is characterized by the volume of trapped air, FV_0, immediately after shaking (at $t = 0$), while the foam stability is characterized by the volume of entrapped air, still remaining in the foam after a certain period of time, $t > 0$.

All foam tests were performed at least twice. Reproducibility of the results was typically ±10%.

2.3. Dynamic surface tension

We measured the dynamic surface tension, $\sigma(t)$ by applying a drop shape analysis of pendant bubble formed in the protein solution. The measurements were performed by using DSA1 software and the Easydrop (Krüss GmbH, Germany). The bubbles were formed by using U-shaped metal needle attached to a syringe and dipped into a glass cuvette with the protein solution. Reproducibility of the $\sigma(t)$ curves was within ±0.5 mN/m for the same ageing time.

2.4. Protein adsorption and $\pi_s(\Gamma)$ isotherms

We performed series of experiments on measuring the adsorption, Γ. Ellipsometry was applied to measure the adsorption of the protein on water/air surface. The used instrument is a modification (Russev et al., 2000) of a conventional null type ellipsometer (LEF 3M, Novosibirsk, Russia), which is adapted for kinetic measurements with time resolution of 1 s. The system works with a solid state laser ($\lambda = 532$ nm, Compass 215M, Coherent, USA) equipped with a light polarizer. All experiments are performed at 50 degrees angle of incidence, which is close to the Brewster angle for water, 53.1 degrees.

The experiments were performed as follows: Aqueous phase (without protein) was poured in a Teflon trough (16 × 6 × 1.5 cm) and the zero polarization state was determined. Afterwards the pure aqueous phase was removed and protein solution was loaded in the trough. 30 min after the protein solution loading the surface of the solution was swept by a Teflon barrier. The moment of surface sweeping is taken as the zero time for the adsorption. The kinetics of adsorption was followed during 3 h.

Similar procedure of protein solution loading was applied in a Langmuir trough (Nima, UK) and the kinetics of surface pressure, $\pi_s(t) = \sigma_0 - \sigma(t)$, vs. time during 3 h was measured (σ_0 is the surface pressure of the pure water). Data records $\pi_s(t)$ and $\Gamma(t)$ have been afterwards matched in order to obtain $\pi_s(\Gamma)$ isotherms.

All measurements were repeated at least twice. The typical reproducibility of the adsorption and surface pressure data was ±0.2 mg/m^2 and ±0.5 mN/m respectively.

2.5. Thin foam films

Thin liquid films were formed in a capillary cell (Exerowa & Kruglyakov, 1998) and observed in reflected light in order to obtain information about the equilibrium thickness, h_{eq}, and for the film lifetime. Films with diameter of 200 ± 20 μm were observed in

a glass cell with an inner diameter of 2.6 mm, thus the capillary pressure during these observations was about 40–50 Pa (Ivanov, 1988). Additionally we made several measurements of disjoining pressure isotherms, $\Pi(h)$, by using the porous cell as described by Dimitrova et al. (2001) and Basheva et al. (2006).

2.6. Size and charge of protein aggregates

We determined the hydrodynamic diameter and the zeta-potential of the protein aggregates in the solutions by using a Zetasizer IIC apparatus (Malvern Instruments, UK) utilizing dynamic light scattering and electrophoretic light scattering. The protein aggregates in 0.1 wt% solutions were studied *in situ*.

Typically, the output of an electrophoretic measurement was a histogram of the electrophoretic mobility (or of the recalculated by the Smoluchowski equation ζ-potential (see for example Kralchevsky, Danov, & Denkov, 2008)) with a given mean value and peak half-width of ≈15% of the mean value. The reproducibility of the mean value of the ζ-potential was within ±3 mV. The output from the size measurements was also a histogram with a given mean value and a half-width of ≈30% of the mean value. Reproducibility of the mean value of the size was better than ±30%.

All measurements were performed at room temperature (22–25 °C).

3. Experimental results

3.1. Foamability

3.1.1. Effect of protein concentration, C_p

Fig. 1 shows the foamability obtained in the Foamscan (FC) and in the Bartsch test (FV_0) as a function of Na-cas concentration at natural pH (6.8). Both FC and FV_0 increased with Na-cas concentration up to 0.3–0.4 wt% and beyond that almost no change was seen. The plateau value of FC ≈ 1.2 was measured for all solutions with Na-cas concentration >0.3 wt% at both gas flow rates, 50 and 100 ml/min. FC > 1 means that the entire volume of the sparged gas has been entrapped in the foam, i.e. no bubble coalescence during the foaming process occurs. Overlaid on Fig. 1, is the FV_0 response for β-cas solutions as well. Although Na-cas solutions displayed the lower foamability than β-cas, the foamability dependence on C_p was almost the same.

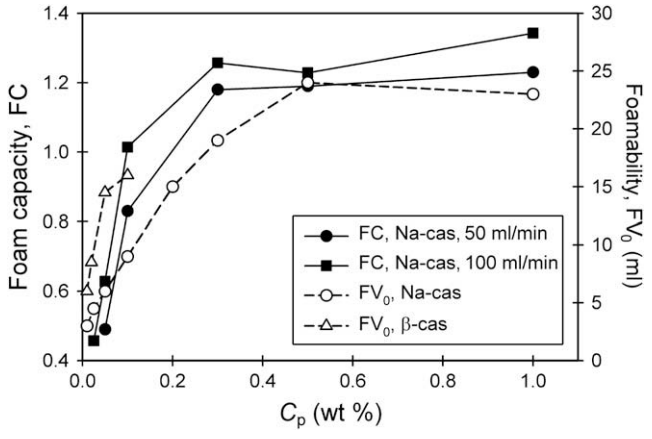

Fig. 1. Foamability FC and FV_0, as determined in the Foamscan and in the Bartsch test, respectively, of Na-cas and β-cas solutions (pH = 6.8, i.e. natural) as a function of the concentration, C_p. FC was determined at two gas flow rates in the Foamscan, as shown on the figure.

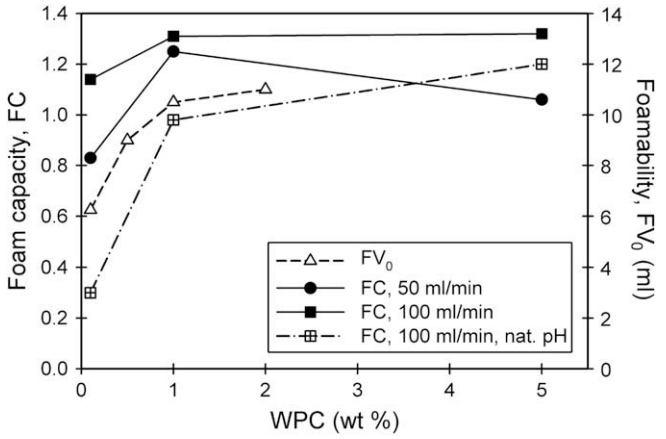

Fig. 2. Foamability measured by the Bartsch test (FV_0) and Foamscan (FC) of WPC solutions as a function of the concentration. pH of the solutions is between 4 and 4.5 except in one of the series (crossed squares).

Fig. 2 compares the foamability obtained by the Foamscan (FC) and the Bartsch test (FV_0) as a function of WPC concentration. As with Na-cas (cf. Fig. 1) both FC and FV_0 increased with protein concentration. However, in the case of WPC its foamability increased with C_p up to 1 wt%, i.e. to much higher concentration than the 0.3 wt% for Na-cas, and beyond that there was little change. Note also that the plateau FV_0 value of WPC (10–11 mL, see Fig. 2) was more than two times smaller than that for Na-cas (22–23 mL, see Fig. 1). Note also that most data on the plot are for solutions with pH between 4 and 4.5, except one of the series (crossed squares), where solutions with natural pH (≈6.4) were used. WPC solutions had best foamability when their pH was near 4 (see the results in the next subsection), that is why most of the presented results for WPC foams were obtained at pH ≈ 4.

Changes in the freshly formed foams with the increase of C_p above the plateau concentration for FC and FV_0 (0.3 wt% Na-cas and 1 wt% WPC) could be followed using the parameter maximum foam density, MD, as seen on Fig. 3. MD is the parameter sensitive to foam wetness and it keeps increasing in the entire concentration range, which witnesses for a continuous increase of the liquid content. The increase of the liquid content is usually related to smaller bubbles (Koehler et al., 2000; Saint-Jalmes et al., 2005; Sanchez & Patino, 2005), and is confirmed by our observations as well (see Fig. 3).

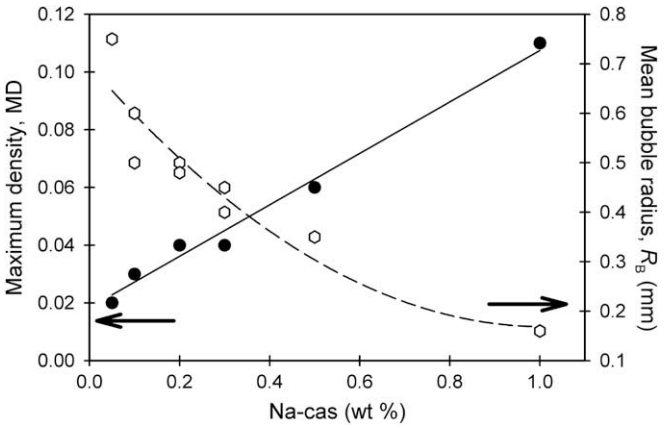

Fig. 3. Maximum foam density, MD (full circles, left ordinate), and mean bubble radius, R_B (empty hexagons, right ordinate), of the foam obtained with Na-cas solutions having natural pH in the Foamscan at gas flow-rate 50 ml/s. The lines are guides to the eye.

As a general feature of the observed foams we could outline that with the increase of C_p there is a stage of fast increase of the foamability followed by a stage where the foamability remains almost constant (and dependent on the method of foam formation) while the bubble size continues to decrease. The concentration, at which the transition occurs is specific for each protein and conditions (e.g. pH). Saint-Jalmes et al. (2005) also have observed S-shaped dependence of the foaming capacity of casein and SDS solutions on the concentration, but their threshold depended on the bubble radius. We did not keep the bubble radius constant, that is why in our experiments the bubble size and the liquid content of the foams kept changing continuously in a wide concentration range in contrast to the foamability.

3.1.2. Effect of pH

We observed very strong pH impact on foamability. Fig. 4A presents data for FV_0 of 0.1 wt% solutions of WPC, WPI and Na-cas as the pH changes from 3 to the natural (6.4–6.8). Na-cas solutions had minimum foamability at the isoelectric pH ($pI_{Nacas} \approx 4.5$). In contrast, both WPC and WPI, exhibited clear foamability maxima at pH = 4. Better foaming of WPC solutions at pH 4.9 than at pH = 9 had previously been observed by Morr (1985) and Lee et al. (1992) for several WPC types.

WPC and WPI are protein mixtures, with each protein having different pI values. Therefore we characterized the "effective" pI by measuring the ζ-potential of protein aggregates present in the WPC solutions. The plot in Fig. 4B presents the measured ζ-potential and size of the aggregates as a function of pH. From pH 4 to 4.5 we detected maximum size of the aggregates and almost zero ζ-potential. Thus we concluded that the effective pI of the selected WPC is between 4 and 4.5, i.e. roughly 4.2. This result shows that the maximum foamability of WPC is around the effective pI (cf. Fig. 4A) in contrast to Na-cas, which has a minimum foamability at pI. Masson and Jost (1986) have measured the ζ-potential of emulsion droplets with WPC and also have determined almost the same pH (4.2) for the potential sign reversal.

The minimum foamability of Na-cas solutions observed near pI might be a consequence of the protein precipitation observed, i.e. there is not enough protein able at adsorbing at the surfaces. On the other hand, the maximum foamability of WPC and WPI near pI witnessed for the minor preventing role due to the precipitation. To check the possible role of the protein precipitation we performed foaming experiments with filtered (with 220 nm pore size filter) 0.1 wt% solutions of Na-cas and of WPC with pH = 4.5. After removing the precipitate, the solution of Na-cas had the same (almost zero) foamability as the non-filtered solution. Notably, the increasing back the pH of the filtered Na-cas solution to the neutral (6.8) restored a significant foamability equal to that of 0.025 wt% Na-cas. This observation shows that there was protein able to adsorb on the surfaces at pI of Na-cas but the adsorption layers could not stabilize the foams.

In contrast, the filtered solution of WPC increased its foaming twice. This observation confirmed the very different role of the precipitated aggregates in the solutions of the two proteins. It suggested also that the precipitated WPC aggregates may have antifoaming effect (Denkov, 2004; Denkov & Marinova, 2006). Still, the different roles of the precipitate between the two protein systems do not explain the opposite foaming tendencies with pH. Different structure of the adsorption layers of the two proteins is rather involved in the explanation of the pH effect on the foaming.

Fig. 5 presents the foamability, FV_0, of 0.1 wt% solutions of the pure proteins BLG and β-cas as a function of pH. The foamability of β-cas solutions did not fully disappear at pI, as observed with Na-cas, however FV_0 changed qualitatively in the same way with pH for both β-cas and Na-cas. This behavior is in agreement with the observations by other authors (e.g. Sanchez & Patino, 2005, and the references therein) that the surface properties of sodium caseinate are dominated and similar to those of β-casein. However the foamability of BLG only slightly increased with pH and there was no distinguishable minima or maxima. This behavior indicates that

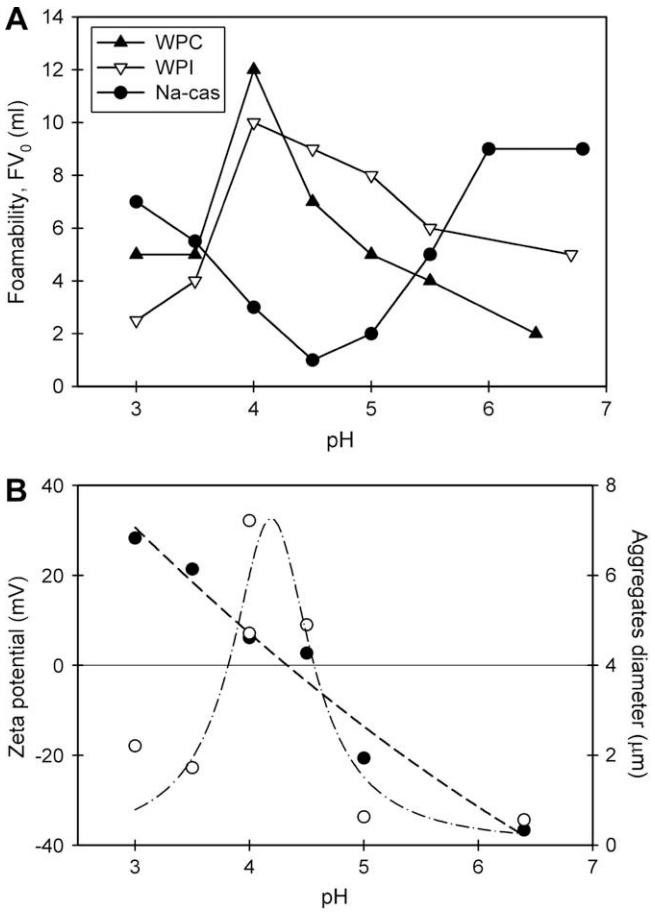

Fig. 4. (A) Foamability, FV_0, vs. pH at 0.1 wt% WPC, WPI and Na-cas solutions. (B) Zeta-potential (full circles, left ordinate) and diameter (empty circle, right ordinate) of protein aggregates as a function of pH of 0.1 wt% WPC solution. The lines are guides to the eye.

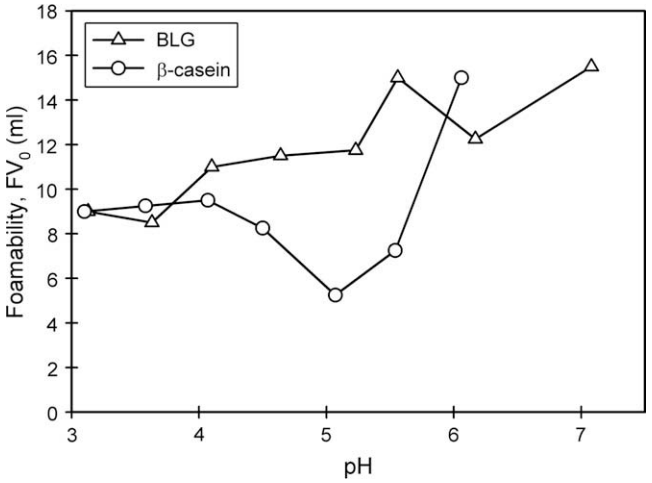

Fig. 5. Foamability, FV_0, vs pH of 0.1 wt% BLG and β-casein solutions.

adsorption and foaming of WPC could not be modeled well by BLG but the effect of the other admixture proteins need to be accounted for as well.

3.1.3. Effect of NaCl

We did not find a substantial effect of NaCl on the foaming of WPC. However Na-cas foams were substantially influenced by the NaCl addition, which was confirmed in both Foamscan and Bartsch tests (see Fig. 6). Addition of 0.15 M NaCl (or more) contributed for significantly better foaming compared to the solutions without NaCl. As will be shown below this correlated well with the rate of surface tension decrease, $-d\sigma/dt$.

For all selected systems the foamability parameters FC and FV_0 changed similarly with the concentrations of protein and salt, and pH of the solutions, regardless of the different regimes of the foam formation, i.e. by bubbling in the Foamscan or by mechanical stirring in the Bartsch method: The foamability increased with the protein concentration, C_p, until a plateau value was reached. Increasing C_p above the plateau value, the foam wetness kept increasing due to the smaller size of the formed bubbles. This result could be very useful when one needs to select a single foam test for a particular task – different numbers could be obtained with the various tests however the dependencies on the concentration of the stabilizer, salt, pH, etc., are expected to be the same.

3.2. Foam drainage and stability

Increasing protein concentration, C_p, leads not only to increasing foamability (e.g. Figs. 1 and 2) but also to an increase in foam stability. Thus we observed that the Na-cas foams at concentrations above 0.1 wt%, and above 0.025 wt% in presence of 150 mM NaCl, were very stable and no destruction had been observed for more than 15 min after foam formation. For the WPC foams we observed substantial destruction with time, especially at natural pH. Fig. 7 shows the foam volume vs. time at natural pH for 1 wt% WPC and 0.1 wt% Na-cas solutions. Foam was created in the Foamscan at a gas-flow rate 100 mL/min. As seen from the plot, Na-cas foam volume increased with a constant rate of ~120 mL/min, while the WPC foam increased with a slower rate (~90 mL/min), i.e. some destruction occurred during the foaming. Consequently the FC was slightly lower than 1 for WPC (see the respective point in Fig. 2). The foam volume from WPC solutions decreased twice for ~3 min ($t_{foam1/2} = 161$ s for the shown sample), while Na-cas foam was very stable for the entire experimental duration (15 min).

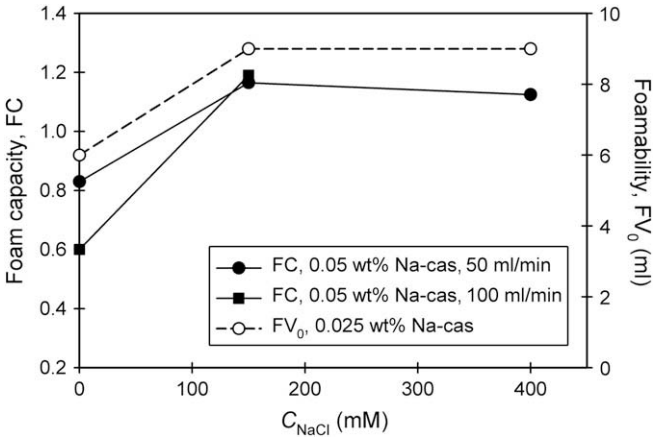

Fig. 6. Foamability, FC and FV_0, vs. concentration of NaCl, C_{NaCl}, in Na-cas solutions having natural pH (6.8).

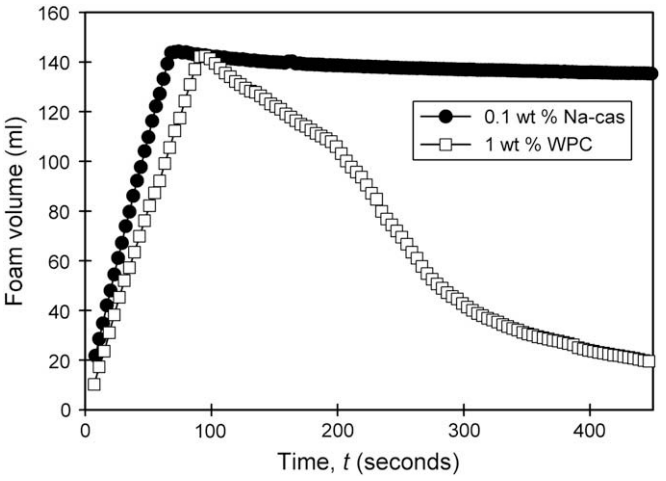

Fig. 7. Foam volume vs time for WPC and Na-cas foams as determined in the Foamscan. The used solutions had natural pH.

Na-cas foam quality was characterized by the drainage behavior. Fig. 8 shows the characteristic drainage time $t_{liq1/2}$ for Na-cas and WPC solutions. Foams obtained at two gas flow-rates are shown. Note that the drainage time of the Na-cas foams is longer when produced at slower gas flow rates. As discussed below, slower gas flow rates favor the higher protein adsorption and lower surface tension, which in turn favors smaller bubbles in the foam, and consequently slower drainage rates. Note that the drainage time of WPC foams was several times shorter than that of Na-cas, which reflected the significant destruction of WPC foams as well.

Furthermore, we plotted the characteristic drainage time, $t_{liq1/2}$, as a function of the inverse square bubble radius (determined 30–60 s after foam formation at a height of 5 cm above the bottom of the foam column) in order to check whether the theoretical predictions are followed: According to the theoretical estimates (Denkov & Marinova, 2006; Koehler et al., 2000) the drainage time, τ_{DR}, should increase as the inverse square of the bubble radius, R_B:

$$\tau_{DR} \sim H_F \left(K_m \rho g R_B^2 \phi_L^m / \eta \right)^{-1} = A R_B^{-2}; \quad m = 1/2 \text{ or } 1 \tag{4}$$

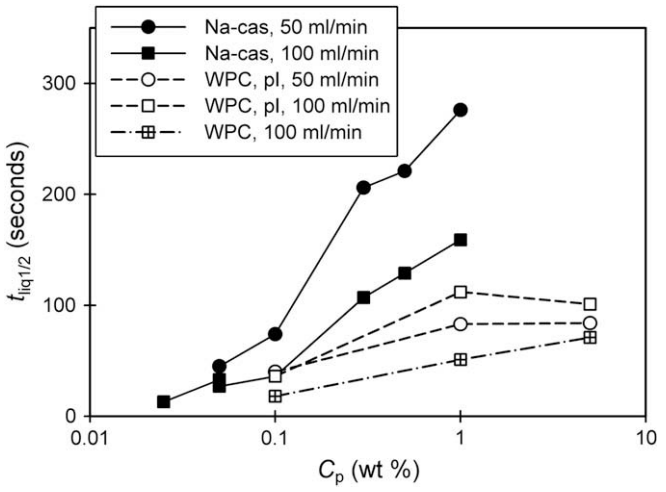

Fig. 8. Time for the liquid in the foam to decrease twice, $t_{liq1/2}$, as a function of the concentration, C_p, of Na-cas and WPC solutions determined in the Foamscan. Solutions have natural pH except in the two series with WPC (empty circles and squares).

where H_F is the foam height, K_m is a numerical constant ($K_1 \approx 6 \times 10^{-3}$ and $K_{1/2} \approx 2 \times 10^{-3}$) and m is a parameter which takes the value of 1 or ½ for tangentially immobile and tangentially mobile surfaces, respectively. As seen from Fig. 9 a good linear dependence is observed between our characteristic drainage time, $t_{liq1/2}$, and R_B^{-2}. From the fit we determined the experimental slope $A = 3.42 \times 10^{-5}$ s/m^2, while the estimate by Eq. (4) gave $A = 3.23 \times 10^{-5}$ s/m^2 for tangentially immobile and $A = 3.07 \times 10^{-5}$ s/m^2 for mobile surfaces (all other parameters were taken typical for the observed by us wet foams: $\phi_L \approx 0.1$, $H_F = 20$ cm, $\rho = 998$ kg m^{-3} and $\eta = 0.95$ cP at 22 °C). The experimental slope is close to the predicted ones, especially to the one for the immobile surfaces and one could conclude that the experimentally observed foam drainage is described satisfactorily with the existing theoretical models (Koehler et al., 2000). Proteins are frequently used (Koehler et al., 2000; Saint-Jalmes et al., 2005) to form foams with tangentially immobile surfaces, which also supports our conclusion for immobile Na-cas surfaces.

3.3. Correlation of the surface and thin films properties with the foaming

3.3.1. Dynamic surface tension

Dynamic surface tension $\sigma(t)$ is expected to be a main determining factor for the foamability (Denkov, 2004; Denkov & Marinova, 2006; Ivanov, 2002; Patino et al., 2008) since the faster rate of decreasing σ directly reflects a faster adsorption, i.e. better stabilization against coalescence. Therefore a series of dynamic surface tension measurements were conducted on WPC and Na-cas solutions at various protein and NaCl concentrations, and pH.

As expected (Dukhin, Kretzschmar, & Miller, 1995; Joos, 1999; Kralchevsky et al., 2008; Patino et al., 2008), we observed that $\sigma(t)$ decreased faster with increasing the protein concentration for both Na-cas and WPC (at all selected pH values and electrolyte concentrations). Fig. 10A illustrates the effect of C_p with curves $\sigma(t)$ for three Na-cas concentrations (natural pH). We determined the values of the initial slopes of the curves, (i.e. $-d\sigma/dt|_{t=0}$, see Fig. 10A) in order to characterize the rate of surface tension decrease when a new surface is created (as it is during the foaming process). Fig. 10B presents the plot of Na-cas and WPC solution foamability as a function of the determined initial slope of $\sigma(t)$. Very good correlation is observed: FC and FV_0 increase almost linearly with the increase of $-d\sigma/dt|_{t=0}$ as C_p increases (e.g. Figs. 1 and 2) and as pH changes, especially for WPC (see Fig. 4A).

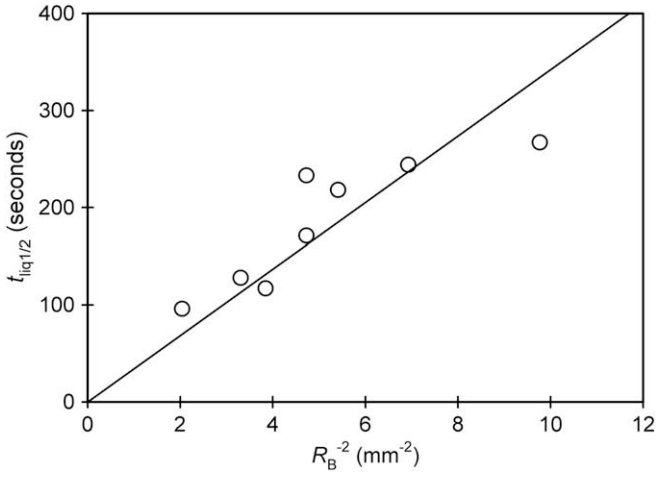

Fig. 9. Correlation plot of $t_{liq1/2}$ vs the inverse square mean bubble radius as measured 50 s after the foam formation from Na-cas solutions. The fit line has a slope 3.42×10^{-5} s/m^2, which is very close to the theoretical prediction 3.23×10^{-5} s/m^2 (calculated by using Eq. (4)) for tangentially immobile surfaces.

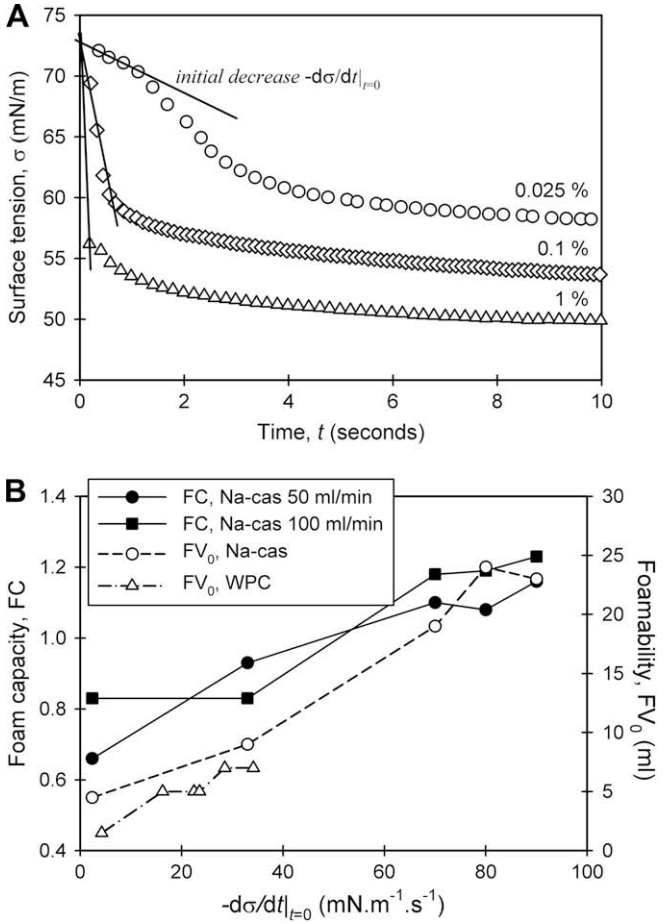

Fig. 10. (A) Dynamic surface tension of Na-cas solutions (natural pH). (B) Foamability of Na-cas and WPC solutions having different concentrations (squares, diamonds, circles) and pH (triangles) measured in the Foamscan (FC, full symbols) and in the Bartsch tests (FV_0, empty symbols) as a function of the rate of initial decrease of the dynamic surface tension, $-d\sigma/dt|_{t=0}$, taken as illustrated in (A).

Increasing the salt concentration is also expected to accelerate adsorption, i.e. to accelerate the dynamic surface tension decrease, especially at pH far from pI since addition of salt is known to screen the electrostatic repulsion between the molecules (see e.g. Dukhin et al., 1995; Kralchevsky et al., 2008; Möbius & Miller, 1998; Tcholakova et al., 2006). Our measurements confirmed this trend: the addition of 150 mM NaCl led to much faster decrease of σ (and to lower values) as compared to the solutions without NaCl for both Na-cas and WPC. The $\sigma(t)$ curves measured in presence of 400 mM NaCl do not differ substantially from those in presence of 150 mM NaCl.

One could calculate the characteristic length of the electrostatic repulsion using the formula (Israelachvili, 1992):

$$\kappa^{-1} = 0.304\, C_{el}^{-1/2}\,\text{nm} \qquad (5)$$

for 1:1 electrolyte with a concentration C_{el} mol/l in water at room temperature. In absence of added NaCl in the solutions the ionic strength is created mainly by the dissociation of the preservative 0.1 g/l NaN_3, i.e. $C_{el} \approx 1$ mM and using Eq. (5) one calculates $\kappa^{-1} \approx 9.6$ nm, which is several times larger than the diameter of the protein molecules (typically 2–3 nm, see e.g. Möbius & Miller, 1998; Gurkov et al., 2003). Upon addition of 150 or 400 mM NaCl κ^{-1}

decreases respectively to ca. 0.8 or 0.5 nm, which is already smaller than the molecular diameter and thus no distinguishable electrostatic adsorption barrier would exist, which explains the faster adsorption and surface tension decrease. On the other hand the electrostatic repulsion does not differ much in presence of 150 or 400 mM NaCl, which also correlates with the dynamic surface tension and foam behavior with Na-cas (e.g. Fig. 6). Note however that the addition of NaCl did improve the foaming with Na-cas while those of WPC did not, i.e. in the case of WPC the faster dynamic surface tension decrease by NaCl did not contribute for improvement of foaming.

We measured the dynamic surface tension of WPC and Na-cas solutions near their pI values in presence of 150 and 400 mM NaCl and we did not detect any significant difference to the case in absence of NaCl. This result had to be expected since the molecules were not charged near pI and there was no electrostatic barrier for adsorption at any electrolyte concentration.

3.3.2. *Protein adsorption and surface elasticity*

We performed series of ellipsometric experiments aimed at measuring directly the adsorption, Γ, of Na-cas and WPC when varying the pH, the protein and NaCl concentration, i.e. the factors that have been found to affect the foaming behavior.

The plots in Figs. 11A and 12A present the kinetics of adsorption, $\Gamma(t)$, from solutions of 0.001 wt% Na-cas and 0.01 wt% WPC respectively. We compared the adsorption at the natural pH to that

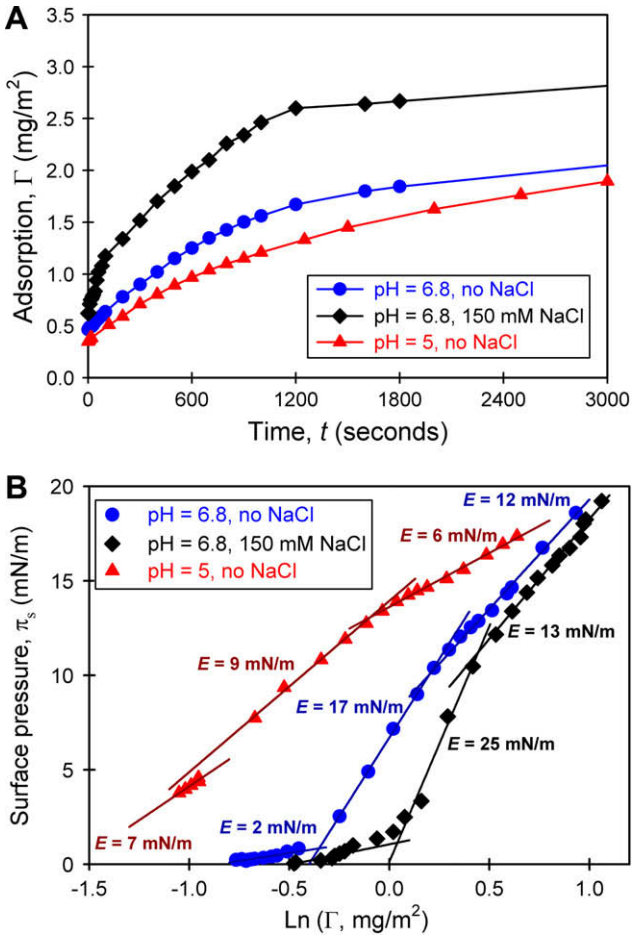

Fig. 11. (A) Adsorption, G, vs. time, t, for 0.001% Na-cas solutions at natural (6.8) and near to the isoelectric pH. (B) Surface pressure π_s vs. lnG for the same solutions. The slopes of the dependencies give the elasticity, E, at given G (see Eq. (6)).

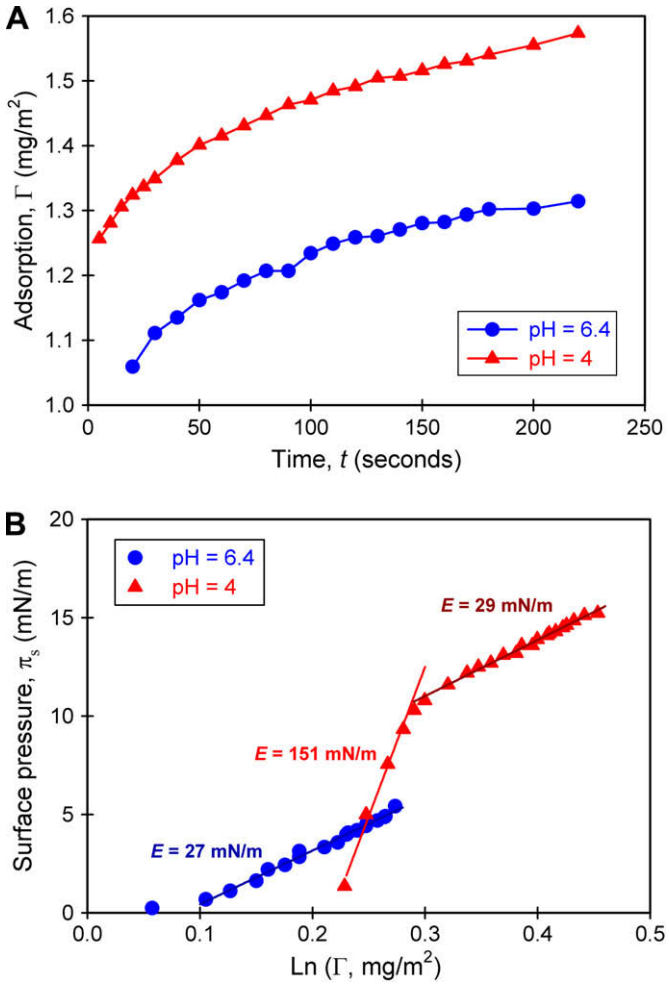

Fig. 12. (A) Adsorption, G, vs. time, t, for 0.01% WPC solutions at natural (6.4) and near to the isoelectric pH. (B) Surface pressure π_s vs. ln G for the same solutions. The slopes of the dependencies give the elasticity, E, at given G (see Eq. (6)).

near to the isoelectric one. Opposite trends were observed for the two proteins: Na-cas adsorption was higher at the natural pH as compared to pI, and especially when NaCl was added (Fig. 11A). In contrast, WPC formed denser adsorption layers near the isoelectric pH than at the natural pH (Fig. 12A). The opposite adsorption trends with the pH correlated well with the observed foaming behavior (cf. Fig. 4A), i.e. the foaming improved when the adsorption increased.

Data for the adsorption, Γ, and the surface pressure, π_s, were taken at the same time-scale and were used to construct experimental $\pi_s(\Gamma)$ isotherms, shown in Figs. 11B and 12B for Na-cas and WPC, respectively. The isotherms are presented as plots of the surface pressure vs. the logarithm of the adsorption in order to calculate directly (from the slope) the elasticity of the layers using the relation:

$$E = d\pi_s/d\ln\Gamma. \quad (6)$$

The calculated values of E are shown on the plots in Figs. 11B and 12B. These values are very close to those measured by the oscillating pendant drop method or with oscillating barriers in a Langmuir trough (Benjamins et al., 1996; Dickinson, 1999; Dickinson & Patino, 1999; Freer, Yim, Fuller, & Radke, 2004; Patino et al., 2008). There have been many attempts in the literature to relate short or long-term foam and emulsion stability to the surface elasticity and/or viscosity: For example, changes in the foamability have been

correlated for some systems with values of the effective elasticity forces (Malysa, Miller, & Lunkenheimer, 1991) and dynamic dilatational elasticity was considered as responsible for foam film stability (Stubenrauch & Miller, 2004). However, most of the authors have concluded that hardly a direct relation could be found (Acharya, Gutiérrez, Aramaki, Aratani, & Kunieda, 2005; Croguennec, Renault, Bouhallab, & Pezennec, 2006; Martin et al., 2002; Patino et al., 2008; Tcholakova et al., 2006). If we have to find some relation from our data it would be also rather controversial: e.g., proteins having lower surface elasticity (Na-cas) have much better foaming and foam stability, however, the factors contributing to the surface elasticity of Na-cas adsorption layers (e.g. addition of salt, change of pH) improve its foaming. Thus our data also do not show a direct correlation between the value of the surface elasticity of the studied proteins and their foaming ability. Other factors such as adsorbed layer structure and interactions between molecules and between adsorbed layers should also be considered in explaining protein foaming. It is worth noting that despite the absence of a direct relation between the value of surface elasticity and foam stability evident from our and from literature data (Acharya et.al., 2005; Croguennec et al., 2006; Martin et al., 2002; Patino et al., 2008), the surface elasticity has been convincingly shown to impact foam drainage (Koehler et al., 2000; Saint-Jalmes et al., 2005) and foam rheology (Denkov, Subramanian, Gurovich, & Lips, 2005; Tcholakova, Denkov, Golemanov, Ananthapadmanabhan, & Lips, 2008).

3.3.3. Thin liquid films

Foams stability is closely related to the stability of the corresponding thin liquid films separating the dispersed gas bubbles (Denkov, 2004; Exerowa & Kruglyakov, 1998; Ivanov, 1988, 2002). That is why we performed model experiments with single foam films with Na-cas and WPC, aimed at understanding the impact of C_p, C_{NaCl}, and pH on the stability and the thickness of the films.

3.3.3.1. Effect of protein concentration. We formed films from solutions with natural pH containing 0.01, 0.1 and 0.5 wt% protein. The measured lifetime and thickness are presented in Table 1. Na-cas films were very stable in the entire concentration range, while those of WPC ruptured in less than 2 min even at the highest concentration used (0.5 wt%). This film behavior was fully consistent with the observed foam stability at natural pH: very stable foams with Na-cas and low foamability and poor stability of WPC foams (cf. Section 3.1.1 above and the figures therein).

3.3.3.2. Effect of NaCl. The addition of NaCl had a different impact on the thickness and stability Na-cas and WPC films, that is why the films with the two proteins are discussed separately below.

To specifically illustrate the effect of NaCl on the Na-cas films we performed systematic measurements with 0.025 wt% protein and different salt concentrations. The measured lifetime and h_{eq} are presented in Table 2. The film thickness gradually decreased from 75 to 45 nm upon increasing the NaCl concentration from 0 to 150 mM, while film stability did not change (the films were very stable, with lifetime >15 min). We also observed a gradual increase of the film thickness inhomogeneity with NaCl concentration, i.e. more aggregates remained entrapped in the films, as C_{NaCl} increased. Such aggregation was observed with WPC films as well (see below) and it was related to the screened repulsion between the protein molecules upon salt addition, which facilitated aggregation.

Table 1
Lifetime and thickness, h_{eq}, of thin foam films with Na-cas and WPC (at natural pH) formed in the capillary cell.

Protein, wt %	WPC		Na-cas	
	Lifetime, seconds	h_{eq}, nm	Lifetime, seconds	h_{eq}, nm
0.01	<10	>100	>900	70–80
0.1	≤60	60–70	>900	60–70
0.5	≤90	80–90	–	–

Table 2
Thickness and lifetime of thin foam films from 0.025 wt% Na-cas solution (natural pH) containing different amounts of NaCl, as determined in the capillary cell. Slope $-\mathrm{d}(\ln \Pi)/\mathrm{d}h$ shown in the forth row was determined from experiments in the porous cell. The values in the last row are the slopes calculated according DLVO theory, by using Eq. (5).

C_{NaCl}, mM	0	10	50	150
h_{eq}, nm	75	60	45–60 (inhomogeneous)	45–60 (inhomogeneous)
Lifetime, s	>900	>900	>900	>900
κ from the slope-$\mathrm{d}(\ln\Pi)/\mathrm{d}h$, nm^{-1}	0.1	0.29	0.22 ± 0.1	0.15 ± 0.1
Theoretical value of κ from Eq. (5), nm^{-1}	0.1	0.33	0.75	1.05

We measured the disjoining pressure isotherms $\Pi(h)$ using the porous cell (Basheva et al., 2006). The determined experimental slopes $-\mathrm{d}(\ln \Pi)/\mathrm{d}h$ are given in the third row of Table 2. If the repulsion between the surfaces were mainly electrostatic, according to the DLVO theory the disjoining pressure would be described by the formula (see e.g. Israelachvili, 1992; or Kralchevsky et al., 2008):

$$\Pi_{el} = 64C_e \cdot N_A \cdot k_B T \gamma^2 e^{-\kappa h}; \quad \gamma = \tanh(e\psi_0/4k_B T), \tag{7}$$

where C_e is the concentration of electrolyte, $N_A = 6.022 \times 10^{23}$ is the Avogadro number, $k_B T$ is the thermal energy, e is the electronic charge, and ψ_0 is the surface potential. For a symmetric monovalent electrolyte κ is given by Eq. (4). Logarithm of Eq. (7) allows one to check directly whether the experimental data can be described as electrostatic repulsion by comparing the slope of the experimental dependence $\ln\Pi$ vs. h to κ calculated by Eq. (4). Last rows of Table 2 contain the experimentally determined slopes and the theoretically expected ones. As seen from the table, at low electrolyte concentration, e.g. up to 10 mM, the experimental and the theoretical slopes are almost identical. The same conclusion has been made by Dimitrova et al. (2001) for β-casein stabilized emulsion films containing 1 mM NaCl. However with 50 and 150 mM NaCl the experimental slopes were almost 4 and 10 times, respectively, smaller that the expected one, i.e. the repulsion between the adsorbed Na-cas layers could not be described by Eq. (7).

Thus the analysis of the disjoining pressure isotherms with Na-cas showed that the foam improving effect of NaCl, especially at high salt concentrations (see Fig. 6), cannot be simply explained with the classical DLVO theory, i.e. with electrostatic repulsion only. Other factors, e.g. steric/osmotic stabilization, are to be involved.

WPC films had a lifetime of less than 2 min at natural pH and NaCl addition did not extend it. An increase of the average thickness of the films was observed in presence of NaCl, however, this effect was probably due to the increased number of protein aggregates trapped in the films, see the pictures in Fig. 13.

In order to explore the effect of aggregates on the film properties we formed films from filtered (with 220 nm pore size filter) 0.5 wt% WPC solution and observed a tremendous increase in their stability. Improved WPC film stability, as well as improved foam stability (as discussed above) after filtration confirmed the possible antifoam effect of the WPC aggregates. Filtered Na-cas solutions produced foam films, which were only slightly thinner and with similar stability to the films formed with the non-filtered solutions. Thus the observed antifoam effect was a specific property of the aggregates in the WPC solutions only. We have not performed any additional studies to clarify further whether the antifoaming was

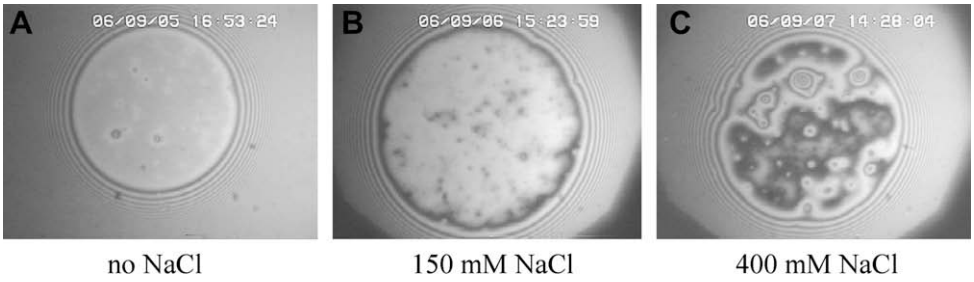

Fig. 13. Images of foam films from 0.1% WPC solution in presence of different concentration of NaCl. Film diameter is ≈ 200 μm.

a property of the particular WPC type but this could be a subject of further studies (as those by Holt et al., 1999; Morr, 1985).

3.3.3.3. Effect of pH. Fig. 14 shows the film lifetime dependence on pH of 0.1 wt% WPC solutions with overlays of its foamability, FV_0, and the rate of surface tension decrease, $-d\sigma/dt|_{t=0}$. Clear correlation is seen between the film stability, foamability and the σ decrease: between pH 4 and 4.5 the films were stable, surface tension decreased faster and the foamability was maximum. Outside of this pH region no stable foams and films were observed, and surface tension decreased slowly. One possible explanation for the highest stability near pI was the formation of denser adsorption layer with minimal electrostatic repulsion between the molecules in the adsorbed layer. Recalling that WPC is a protein mixture with different pI values the highest stability in this region could be related to some special compositional effect within the adsorbed layer under specific conditions.

For Na-cas films pH effect was contrary to those observed with WPC (similarly to observations with the foams, Fig. 4A). The films from 0.01 wt% Na-cas solutions at pH = 6.8 were very stable in contrast to those at pH = 5, where very fast film rupture occurred. The film stability increased when increasing the concentration from 0.01 to 0.1 wt% at all pH values.

In summary all measurements showed full correlation between the lifetime of the thin films of Na-cas and WPC with pH and C_p and the respective foamability – maximum film and foams stability with WPC at pH between 4 and 4.5 (near pI); unstable films and foams from Na-cas at pH between 4 and 5 (near pI).

4. Discussion

4.1. Common features of the foaming of milk protein solutions

The performed systematic foaming tests and experiments with single interfaces (e.g. surface tension, adsorption, and thin films) showed several common properties of the selected milk protein systems: (i) Increase of the protein concentration, C_p, led to increasing in the foamability to an almost constant value after some threshold concentration. (ii) Increase of C_p led to increased adsorption and faster dynamic surface tension decrease, and to longer thin film lifetime. (iii) Addition of NaCl led to faster dynamic surface tension decrease and higher adsorption when pH was different from pI, and to a significant aggregation of the proteins, as observed in the thin films. (iv) Increased adsorption, as detected in the ellipsometric measurements, always correlated with a higher foamability. All these common properties were to be expected since both the concentration of the stabilizer and the concentration of salt (when added to charged stabilizer) are known to contribute for faster and larger adsorption, i.e. to higher surface coverage and better stabilization against coalescence (see for example Möbius & Miller, 1998; Patino et al., 2008; Tcholakova et al., 2006).

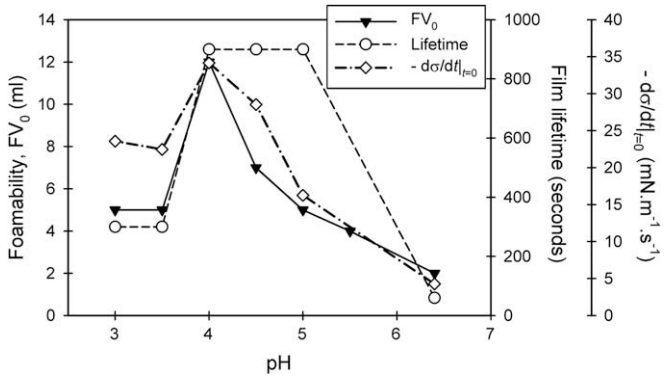

Fig. 14. Film lifetime, foamability, FV_0, and rate of dynamic surface tension decrease, $-d\sigma/dt|_{t=0}$, for 0.1wt% WPC solutions as a function of pH.

The Foamability vs. C_p relationship had the same shape with two different foaming tests, i.e. when the bubbles were formed by sparging (Foamscan) and when the foam was generated by mechanically mixing the liquid with the gas in a closed cylinder (Bartsch test). Operating the Foamscan apparatus at low gas flow rates one could model the process of bubble formation as a quasi-static process (Exerowa & Kruglyakov, 1998; Gerlach et al., 2007; Prud'homme & Khan, 1996). From the balance of the buoyancy and surface tension forces for a quasi-static detachment of a bubble with radius R from a pore of radius r one derives:

$$R = (3\sigma r/(2\rho g))^{1/3} \quad (8)$$

where g is gravity acceleration, σ is the surface tension, and ρ is the density of the liquid. This equation shows that at one and the same pore radius and liquid density, the bubble radius R is determined primarily by the surface tension, σ. When the bubble formation proceeds faster than the surface tension decrease to the equilibrium value, the relevant dynamic surface tension value $\sigma(t)$ should be considered in Eq. (8).

For Foamscan experiments with 0.1 wt% Na-cas Eq. (8) predicts that bubbles with mean radius of 0.6 mm would form from pores with mean radius of 15 μm if the surface tension were ≈ 60 mN/m, i.e. almost 10 mN/m higher that the equilibrium one (see Fig. 10A). The dynamic surface tension of 0.1 wt% Na-cas solution (see Fig. 10A) reaches 60 mN/m for ≈ 0.5 s, i.e. a single bubble would need 0.5 s after the formation to reach this surface tension and to detach. On the other hand one could estimate the formation/detachment time of a single bubble from the particular experimental record: in the 0.1 wt% Na-cas solution 140 mL foam (with 3.9 mL liquid in it) was formed for 242 s, i.e. ≈ 34 mL/min foam bubbles were generated. This total volume corresponds to 630 bubbles/seconds (bubble radius 0.6 mm). If approximately 100 pores were active, the formation time for a single bubble from a pore would be ≈ 160 milliseconds. Thus, the real bubble formation/detachment time turned out to be 3 times shorter than the one

predicted from Eq. (8) and the measured $\sigma(t)$ dependence. A possible explanation for this difference could be found in the strong convection during the bubble generation process – even very low convection might accelerate significantly the adsorption and the surface tension decrease, as shown by Fainerman et al. (2006).

Although approximate and somewhat speculative, the above estimates demonstrate that the correlation between dynamic surface tension and foamability has a firm physico-chemical basis. A rigorous description would be obtained if the convective adsorption and the bubble formation process were better quantified. Besides, the decrease in the radius of the bubbles with the protein concentration (see Fig. 3) also supports the importance of the dynamic adsorption and dynamic surface tension for the bubble formation process.

Foam formation by the Bartsch method cannot be modeled with the "simple" process of bubble detachment from a pore. Viscous stresses rather should be involved to describe the bubble breakup processes (Tcholakova et al., 2008). Although the foam formation processes seems to develop in different regimes with very different factors involved, the same foamability dependence on the protein concentration suggests the existence of common governing factors. One such factor could be the surface coverage of the bubble remaining in the foam. The primary bubbles formed in the two methods (by two different mechanisms) might be very different as size, size distribution, and surface coverage, however all bubbles with low surface coverage will coalesce and only those having the minimum surface coverage ensuring stability will remain stable (Ivanov, 2002; Tcholakova et al., 2006).

4.2. Differences between caseins and whey proteins

Along with the common properties, we observed several significant differences between the foams stabilized with WPC and with Na-cas: (i) at natural pH foaming of Na-cas was very good with very stable foams, in contrast to WPC, which formed significantly less foam with negligible stability. (ii) The addition of NaCl to Na-cas solutions at natural pH further improved its foaming, while no effect on WPC foaming was detected (despite the significant effect on the dynamic surface tension). (iii) upon decreasing the pH from the natural down to 3, the foaming of Na-cas solutions passed through a deep minimum at the isoelectric pI (4.5), while the foaming of WPC (and WPI) passed through a high maximum near the effective pI of ≈4.2. These foamability changes were well correlated with the changes in the thin film lifetimes and the adsorption with pH. The observed similarities and differences suggested that the structure of the formed adsorption layers should be also involved in order to obtain a more general and self-consistent picture of the factors playing role for the foaming in the different cases.

In order to explain consistently the foam properties observed by us, together with those of the single films and surfaces, we constructed a speculative schematic picture (sketched in Fig. 15) of the adsorbed layers (similarly to the approach by Graham & Phillips, 1980, or by Pereira et al., 2003). Since we did not obtain direct information for the structure of the layers in our measurements we have invoked also some information from the literature.

It is accepted in the literature that the surface properties of caseinates are determined by β-casein predominantly. The similar pH dependences of the foamability of Na-cas and β-casein observed by us confirmed this observation. Furthermore, our Na-cas surface pressure isotherms were nearly identical to those of β-casein from Graham and Phillips (1980) (detailed comparison of these data is included in a forthcoming manuscript (Ivanov, Mirarefi, & Campbell, in preparation)). Therefore we modeled the Na-cas adsorption layers by treating them as β-casein ones. The β-casein polypeptide

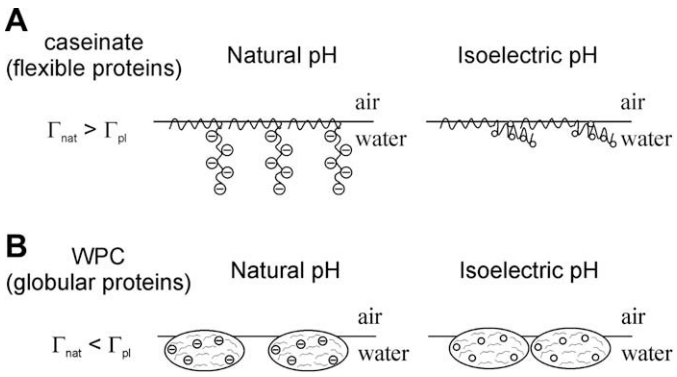

Fig. 15. Schematic presentation of Na-cas (A) and WPC (B) and molecules adsorbed at water/air surface.

has 209 amino acid residues; the first 50 are predominantly hydrophilic, while the remaining 159 residues are predominantly hydrophobic (Dickinson, 1999). Neutron reflectivity studies (Dickinson, 1999; Dickinson et al., 1993) have shown that the adsorbed layer of β-casein molecules can be represented as an inner dense layer of thickness 1–2.5 nm adjacent to the interface, and an outer less dense layer, extending 3–7.5 nm further into the aqueous phase. The inner layer is accepted to be composed mostly from the hydrophobic amino-residues in a "train" configuration, while the hydrophilic chain extends farther away as a "tail" or "loop" (Dickinson et al., 1993). Accordingly we present the adsorption layer of casein as shown in Fig. 15A. One could see that the large distance between the hydrophilic residues of the molecules would allow the electrolyte counterions to easily penetrate in between the chains and thus to screen very effectively the electrostatic repulsion between the molecules in the adsorption layer. The depicted structure would allow such compaction to be realized even at minor screening electrolyte in the aqueous phase (e.g. 1 mM ensured by the added 0.1 g/l NaN_3) since the distance between the hydrophilic chains is large anyway due to the large area occupied by the hydrophobic segments at the surface. The change in the adsorption layer at the pI could be interpreted in various ways since there is no direct structural information available. We would rely on our ellipsometric measurements which showed that the adsorption is higher at pI as compared to the natural pH. That is why we have accepted that the hydrophilic residues, which are not charged at the pI shrink slightly to the surface and the area per molecule increases slightly accordingly (Fig. 15A). Thus we would speculate that the decreased foamability at the isoelectric pH is not due to the casein precipitation only but to lower surface coverage and weaker repulsion between the thin film surfaces, which cannot ensure enough film and foam stabilization.

Modeling the adsorption layers of WPC and WPI with a single protein is quite controversial, although its major protein is β-lactoglobulin (Holt et al., 1999). Several authors in different studies have shown that the surface properties of whey concentrate are different from those of β-lactoglobulin. Our foaming experiments also showed different foamability dependence on pH for WPC and β-lactoglobulin. Zhang, Dalgleish, and Goff (2004) recently have shown that a change in the proportions of β-lactoglobulin to α-lactalbumin (the second major protein in the whey concentrates) in the foams with WPC might occur with pH. Whatever the particular surface composition is, the adsorption layer is composed of globular proteins. That is why we are speculating that the adsorbed layer from the whey protein mixture is composed of an "average" globular protein (see Fig. 15B). This "average" globular protein molecule adsorbs almost intact at the interface, at least initially (Freer et al., 2004; Gurkov et al., 2003). At its natural pH the

molecule is negatively charged and the electrostatic repulsion prevents the formation of a very dense adsorption layer. Upon salt addition the adsorbed monolayer might increase slightly but not significantly since some of the charged amino-acids could be inaccessible for effective electrostatic screening. At the "effective" pI the molecules are not charged and its adsorption is highest. Our proposed model does not contradict the observation by Zhang et al. (2004) that some compositional change in the adsorbed layer may occur. β-lactoglobulin has pI = 5.2 and α-lactalbumin has pI between 4.1 and 4.8, and thus consistent with our effective pI = 4.2. If the adsorption layer at the effective pI were composed of slightly positively charged β-lactoglobulin and slightly negatively charged α-lactalbumin this would further strengthen the compaction of the molecules and the high adsorption would prevent the rupture of the thin films and would ensure a high foamability.

Although explaining many of our observations the proposed pictorial model could be significantly refined and improved after having more quantitative data for the variations of the properties of the adsorption layers with pH, e.g. structural information for the adsorption layers as those by Dickinson et al. (1993) and by Chakraborty and Basak (2007). Alternatively quantitative information could be obtained from the precise quantitative description of the adsorption isotherms with suitable equation of state (Ivanov et al. in preparation).

5. Conclusion

The performed systematic foaming tests with caseins and globular whey proteins solutions showed that for all studied systems the foamability changed in a similar manner with the concentrations of protein and salt, and pH, regardless of the regime of foam formation, i.e. by bubbling in the Foamscan or by mechanical agitation in the Bartsch method. For all used proteins the foamability increased with the protein concentration, C_p, until a plateau value was reached. Upon increasing C_p above the plateau value, the foam wetness kept increasing due to the decreasing size of the formed bubbles.

The foamability of WPC was maximum near the effective pI in contrast to sodium caseinate which foamability was minimum near pI. The opposite foaming tendencies correlated well with the measured change of the adsorption and with the observed variation of the stability of the thin films with pH.

Good correlation was observed between the foamability and the rate of surface tension decrease $-d\sigma/dt|_{t=0}$, as C_p and pH change. WPC foaming correlated well with $-d\sigma/dt|_{t=0}$ as pH changed from 3 to 6.4, but this correlation was lost when salt was added to the solutions at the natural pH.

The most probable explanation for the differences in the stability of the films and foams of the two protein types were the different molecular structure and different aggregation behavior. Speculative pictorial model of the adsorption layers based on the structural data available from the literature was proposed to explain the foam and surface properties observed by us: Casein adsorption layers are denser and thicker and ensure better stabilization far from the isoelectric pI. Added electrolyte increased further the adsorption and the repulsion between the surfaces (probably by steric and/or osmotic mechanism). In contrast, the globular molecules of WPC probably could not compact well to ensure the necessary films and foams stabilization far from pI, even after electrolyte addition. Thus the increase of protein concentration at neutral pH led to better foaming for Na-caseinate than for WPC.

Aggregation of WPC near the effective pI could not deplete the protein available for adsorption on the surfaces but the formed aggregates exhibit antifoam effect. We observed almost double increase of the foamability upon removal of precipitated aggregates.

New detailed quantitative information for the structure of the adsorption layers obtained either experimentally or by appropriate theoretical description of the available data for the adsorption will help further to explain at a deeper mechanistic level the observed trends.

Acknowledgments

This study was supported by Kraft Foods, Glenview, IL. The authors are indebted to Prof. N. Denkov for the helpful discussions.

References

Acharya, D. P., Gutiérrez, J. M., Aramaki, K., Aratani, K., & Kunieda, H. (2005). Interfacial properties and foam stability effect of novel gemini-type surfactants in aqueous solutions. *Journal of Colloid and Interface Science, 291*, 236–243.

Bartsch, O. (1924). Uber Schaumsysteme. *Fortschrittsberichte über Kolloide und Polymere, 20*, 1–49.

Basheva, E. S., Gurkov, T. D., Christov, N. C., & Campbell, B. (2006). Interaction in oil/water/ oil films stabilized by β-lactoglobulin; role of the surface charge. *Colloids Surfaces A: Physicochemical and Engineering Aspects, 282–283*, 99–108.

Benjamins, J., Cagna, A., & Lucassen-Reynders, E. H. (1996). Viscoelastic properties of triacylglycerol/water interfaces covered by proteins. *Colloids Surfaces A: Physicochemical and Engineering Aspects, 114*, 245–254.

Bikerman, J. J. (1973). *Foams*. Berlin: Springer-Verlag.

Chakraborty, A., & Basak, S. (2007). pH-induced structural transitions of caseins. *Journal of Photochemistry and Photobiology B: Biology, 87*(3), 191–199.

Creamer, L. K., & MacGibbon, A. K. H. (1996). Some recent advances in the basic chemistry of milk proteins and lipids. *International Dairy Journal, 6*(6), 539–568.

Croguennec, T., Renault, A., Bouhallab, S., & Pezennec, S. (2006). Interfacial and foaming properties of sulfydryl-modified bovine β-lactoglobulin. *Journal of Colloid and Interface Science, 302*(1), 32–39.

Denkov, N. D. (2004). Mechanisms of foam destruction by oil-based antifoams. *Langmuir, 20*(22), 9463–9505.

Denkov, N. D., & Marinova, K. G. (2006). Antifoam effects of solid particles, oil drops and oil-solid compounds in aqueous foams. In B. P. Binks, & T. S. Horozov (Eds.), *Colloidal particles at liquid interfaces* (pp. 383–444). Cambridge: Cambridge University Press.

Denkov, N. D., Subramanian, V., Gurovich, D., & Lips, A. (2005). Wall slip and viscous dissipation in sheared foams: effect of surface mobility. *Colloids Surfaces A: Physicochemical and Engineering Aspects, 263*(1–3), 129–145.

Dickinson, E. (1999). Review: adsorbed protein layers at fluid interfaces: interactions, structure and surface rheology. *Colloids and Surfaces B: Biointerfaces, 15*(2), 161–176.

Dickinson, E., Horne, D. S., Phipps, J. S., & Richardson, R. M. (1993). A neutron reflectivity study of the adsorption of beta-casein at fluid interfaces. *Langmuir, 9*(1), 242–248.

Dickinson, E., & Patino, J. M. R. (1999). *Food emulsions and foams – Interfaces, interactions and stability*. London: RSC. Spec. Ed. № 227.

Dimitrova, T. D., Leal-Calderon, F., Gurkov, T. D., & Campbell, B. (2001). Disjoining pressure vs thickness isotherms of thin emulsion films stabilized by proteins. *Langmuir, 17*(26), 8069–8077.

Dukhin, S. S., Kretzschmar, G., & Miller, R. (1995). *Dynamics of adsorption at liquid interfaces*. Amsterdam: Elsevier.

Exerowa, D., & Kruglyakov, P. M. (1998). *Foams and foam films: Theory, experiment, application*. Amsterdam: Elsevier.

Fainerman, V. B., Lylyk, S. V., Ferri, J. K., Miller, R., Watzke, H., Leser, M. E., et al. (2006). Adsorption kinetics of proteins at the solution/air interfaces with controlled bulk convection. *Colloids Surfaces A: Physicochemical and Engineering Aspects, 282–283*, 217–221.

Freer, E. M., Yim, K. S., Fuller, G. G., & Radke, C. J. (2004). Interfacial rheology of globular and flexible proteins at the hexadecane/water interface: comparison of shear and dilatation deformation. *The Journal of Physical Chemistry B, 108*(12), 3835–3844.

Gerlach, D., Alleborn, N., Buwa, V., & Durst, F. (2007). Numerical simulation of periodic bubble formation at a submerged orifice with constant gas flow rate. *Chemical Engineering Science, 62*(7), 2109–2125.

Graham, D. E., & Phillips, M. C. (1979). Proteins at liquid interfaces III. Molecular structures of adsorbed films. *Journal of Colloid and Interface Science, 70*(3), 427–439.

Graham, D. E., & Phillips, M. C. (1980). Proteins at liquid interfaces IV. Dilatational properties. *Journal of Colloid and Interface Science, 76*(1), 227–239.

Gurkov, T. D., Russev, S. C., Danov, K. D., Ivanov, I. B., & Campbell, B. (2003). Monolayers of globular proteins on air/water interface: applicability of the volmer equation of state. *Langmuir, 19*(18), 7362–7369.

Holt, C., McPhail, D., Nylander, T., Otte, J., Ipsen, R. H., Bauer, R., et al. (1999). Some physico-chemical properties of nine commercial or semi-commercial whey

protein concentrates, isolates and fractions. *International Journal of Food Science & Technology, 34*(5–6), 587–601.
Israelachvili, J. N. (1992). *Intermolecular and surface forces* (2nd ed.). New York: Academic Press.
Ivanov, I. B. (1988). *Thin liquid films: Fundamentals and applications*. New York: Marcel Dekker.
Ivanov, I. B. (2002). *Plenary lecture in the symposium surfactants in solutions*. Barcelona: Spain.
Ivanov, I. B., Mirarefi, A., & Campbell, B. Equation of state of caseinate monolayers and stability of thin films. Manuscript based on a lecture in the symposium surfactants in solutions, 2008, Berlin, Germany, in preparation.
Joos, P. (1999). *Dynamic surface phenomena*. The Netherlands: VSP BV, AH Zeist.
Koehler, S. A., Hilgenfeldt, S., & Stone, H. A. (2000). A generalized view of foam drainage: experiment and theory. *Langmuir, 16*(15), 6327–6341.
Kralchevsky, P. A., Danov, K. D., & Denkov, N. D. (2008). Chemical physics of colloid systems and interfaces. In *K.S. Birdi handbook of surface and colloid chemistry* (3rd ed.). New York: CRC Press. p. 197.
Lee, S.-Y., Morr, C. V., & Ha, E. Y. W. (1992). Structural and functional properties of caseinate and whey protein isolate as affected by temperature and pH. *Journal of Food Science, 57*(2), 1210–1229.
Makievski, A. V., Fainerman, V. B., Bree, M., Wustneck, R., Kragel, J., & Miller, R. (1998). Adsorption of proteins at the liquid/air interface. *The Journal of Physical Chemistry B, 102*(2), 417–425.
Malysa, K., Miller, R., & Lunkenheimer, K. (1991). Relationship between foam stability and surface elasticity forces: fatty acid solutions. *Colloids and Surfaces, 53*, 47–62.
Marinova, K. G., Gurkov, T. D., Velev, O. D., Ivanov, I. B., Campbell, B., & Borwankar, R. P. (1997). The role of additives for the behaviour of thin emulsion films stabilised by proteins. *Colloids Surfaces A: Physicochemical and Engineering Aspects, 123–124*, 155–167.
Martin, A. H., Grolle, K., Bos, M. A., Cohen Stuart, M. A., & van Vliet, T. (2002). Network forming properties of various proteins adsorbed at the air/water interface in relation to foam stability. *Journal of Colloid and Interface Science, 254*(1), 175–183.
Masson, G., & Jost, R. (1986). A study of oil-in-water emulsions stabilized by whey proteins. *Colloid & Polymer Science, 264*(7), 631–638.
Möbius, D., & Miller, R. (1998). *Proteins at liquid interfaces*. Amsterdam: Elsevier.
Morr, C. V. (1985). Composition, physicochemical and functional properties of reference whey protein concentrates. *Journal of Food Science, 50*(5), 1406–1411.
Murray, B. S. (2007). Stabilization of bubbles and foams. *Current Opinion in Colloid & Interface Science, 12*(4–5), 232–241.
Murray, B. S., & Ettellaie, R. (2004). Foam stability: proteins and nanoparticles. *Current Opinion in Colloid & Interface Science, 9*(5), 314–320.
Patino, J. M. R., Sanchez, C. C., & Nino, M. R. R. (2008). Implications of interfacial characteristics of food foaming agents in foam formulations. *Advances in Colloid and Interface Science, 140*(2), 95–113.
Pereira, L. G. C., Johansson, C., Radke, C. J., & Blanch, H. W. (2003). Surface forces and drainage kinetics of protein-stabilized aqueous films. *Langmuir, 19*(18), 7503–7513.
Prud'homme, R. K., & Khan, S. A. (1996). *Foams: Theory, measurements, and applications*. New York: Marcel Dekker.
Russev, S. C., Arguirov, T. V., & Gurkov, T. D. (2000). Beta-casein adsorption kinetics on air-water and oil-water interfaces studied by ellipsometry. *Colloids and Surfaces B: Biointerfaces, 19*(1), 89–100.
Saint-Jalmes, A., Peugeot, M.-L., Ferraz, H., & Langevin, D. (2005). Differences between protein and surfactant foams: microscopic properties, stability and coarsening. *Colloids and Surfaces A: Physicochemical and Engineering Aspects, 263*(1–3), 219–225.
Sanchez, C. C., & Patino, J. M. R. (2005). Interfacial, foaming and emulsifying characteristics of sodium caseinate as influenced by protein concentration in solution. *Food Hydrocolloids, 19*(3), 407–416.
Stubenrauch, C., & Miller, R. (2004). Stability of foam films and surface rheology: an oscillating bubble study at low frequencies. *The Journal of Physical Chemistry B, 108*(20), 6412–6421.
Tcholakova, S., Denkov, N. D., Golemanov, K., Ananthapadmanabhan, K. P., & Lips, A. (2008). Theoretical model of viscous friction inside steadily sheared foams and concentrated emulsions. *Physical Review E, 78*. 011405.
Tcholakova, S., Denkov, N. D., Ivanov, I. B., & Campbell, B. (2002). Coalescence in β-lactoglobulin-stabilized emulsions: effects of protein adsorption and drop size. *Langmuir, 18*(23), 8960–8971.
Tcholakova, S., Denkov, N. D., Ivanov, I. B., & Campbell, B. (2006). Coalescence stability of emulsions containing globular milk proteins. *Advances in Colloid and Interface Science, 123–126*, 259–293.
Tcholakova, S., Denkov, N. D., Sidzhakova, D., Ivanov, I. B., & Campbell, B. (2005). Effects of electrolyte concentration and pH on the coalescence stability of β-lactoglobulin emulsions: experiment and interpretation. *Langmuir, 21*(11), 4842–4855.
Weaire, D., & Hutzler, S. (1999). *The physics of foams*. Oxford: Clarendon Press.
Zhang, Z., Dalgleish, D. G., & Goff, H. D. (2004). Effect of pH and ionic strength on competitive protein adsorption to air/water interfaces in aqueous foams made with mixed milk proteins. *Colloids and Surfaces B: Biointerfaces, 34*(2), 113–121.